Structural/Functional Characterization of the α_2-Plasmin Inhibitor C-Terminal Peptide†

Pascal S. Frank,‡,§ Justin T. Douglas,‡,|| Michael Locher,§ Miguel Llinás,*,|| and Johann Schaller§

Department of Chemistry and Biochemistry, University of Berne, Freiestrasse 3, CH-3012 Berne, Switzerland, and Department of Chemistry, Carnegie Mellon University, 4400 Fifth Avenue, Pittsburgh, Pennsylvania 15213

Received September 27, 2002; Revised Manuscript Received November 14, 2002

ABSTRACT: The α_2-plasmin inhibitor (A2PI) is a main physiological regulator of the trypsin-like serine proteinase plasmin. It is composed of an N-terminal 15 amino acid fibrin cross-linking polypeptide, a 382-residue serpin domain, and a flexible C-terminal segment. The latter, peptide Asn^{398}−Lys^{452}, and its Lys452Ala mutant were expressed as recombinant proteins in *Escherichia coli* (r-A2PIC and r-A2PICmut, respectively). CD and NMR analyses indicate that r-A2PIC is flexible, loosely folded, and with low content of regular secondary structure. Functional characterization via intrinsic fluorescence ligand titrations shows that r-A2PIC interacts with the isolated plasminogen kringle 1 (r-K1) ($K_a \sim 69.9$ mM^{-1}), K4 ($K_a \sim 45.7$ mM^{-1}), K5 ($K_a \sim 4.3$ mM^{-1}), and r-K2 ($K_a \sim 3.2$ mM^{-1}), all of which are known to exhibit lysine-binding capability. The affinities of these kringles for r-A2PIC are consistently larger than those reported for the ligand N^{α}-acetyllysine, a mimic of a C-terminal Lys residue. The r-A2PICmut, with a C-terminal Ala residue, also interacts with r-K1 and K4, although with approximately 5-fold lesser affinities relative to r-A2PIC, demonstrating that while Lys^{452} plays a major role in the binding, internal residues in r-A2PIC tether the kringles. ^{1}H NMR spectroscopy shows that key aromatic residues within the K4 lysine-binding site (LBS), namely, Trp^{25}, Trp^{62}, Phe^{64}, Trp^{72}, and Tyr^{74}, selectively respond to the addition of r-A2PIC and r-A2PICmut, indicating that these interactions proceed via the kringles' canonical LBS. We conclude that r-A2PIC docks to kringles primarily through lysine side chains and that Lys^{452} most definitely enhances the binding. This suggests that multiple Lys residues within A2PI could contribute, perhaps in a zipper-like fashion, to its binding to the in-tandem, multikringle array that configures the plasmin heavy chain.

Hemostatic avoidance of indiscriminate proteolysis and tissue damage requires precise, coordinated regulation of plasmin (Plm),[1] the key enzyme of the fibrinolytic cascade. Plasminogen (Pgn), the zymogen of Plm, is a multidomain protein that consists of an N-terminal PAN module (*1*), five kringle repeats, and a trypsin-like serine protease unit. The α_2-plasmin inhibitor (A2PI) (previously α_2-antiplasmin), a main physiological regulator of Plm, is a member of the serine protease inhibitor (serpin) superfamily. It induces Plm into cleaving the A2PI reactive site (Arg^{365}-Met^{366}), which results in a covalently bound inactive Plm−A2PI complex of 1:1 stoichiometry (*2*).

A2PI extends approximately 50 amino acids beyond the consensus serpin sequence (*3*), suggesting a distinct and specific function for the C-terminal Asn^{398}−Lys^{452} segment (A2PIC) (Scheme 1), assumedly the binding to plasmin(ogen) kringles (*4*−*6*). Indeed, A2PI inhibits miniplasmin, a Plm fragment possessing only kringle 5 and the fully active protease, approximately 60-fold less rapidly than intact Plm (*7*). Conversely, human plasma contains a partially degraded form of A2PI, comprising up to 30% of the physiological protein content (*8*), that lacks the C-terminal segment and reacts less readily with Plm than native A2PI (*9*). Related to these observations, kinetic studies (*10*, *11*) suggest a two-step model for rapid inhibition of Plm: a fast reversible second-order reaction followed by a slower irreversible first-order process. The latter step represents the cleavage of the A2PI reactive site by the Plm protease module, while the initial second-order process has been ascribed to the forma-

† These studies were supported by the Swiss NSF, Grants 31-45816.95 and 31-52236.97, a grant from the Roche Research Foundation, and NIH Grant HL-29409 from the Department of Health and Human Services.

* Corresponding author. Phone: (412) 268-3134. Fax: (412) 268-1061. E-mail: llinas@andrew.cmu.edu.

‡ P.S.F. and J.T.D. contributed equally to this work.

§ University of Berne.

|| Carnegie Mellon University.

[1] Abbreviations: AcLys, N^{α}-acetyllysine; AcLysOMe, *N*-acetyllysine methyl ester; 6-AHA, 6-aminohexanoic acid; A2PI, human α_2-plasmin inhibitor; A2PIC, C-terminal peptide of A2PI (Asn^{398}−Lys^{452}); CD, circular dichroism; COSY, correlated spectroscopy; EEDY*445, segment 442−445 of A2PI, with sulfonated Tyr^{445}; eu, electric charge unit; ESI-MS, electrospray ionization mass spectrometry; FXa, activated coagulation factor X; PAN, plasminogen N-terminal domain; Pgn, human plasminogen; Plm, human plasmin; His tag, peptide MRGSH-HHHHHGSIEGR; K1, kringle 1 domain of Pgn (Cys^{84}−Cys^{162}), generated as r-K1; K2, kringle 2 domain of Pgn (Cys^{166}−Cys^{243}), generated as r-K2; K3, kringle 3 domain of Pgn (Cys^{256}−Cys^{333}), generated as r-K3; r-K3mut, mutant K3 domain of Pgn (TYQ[K3/C297/S/K311D]DS), generated as r-K3mut; K4, kringle 4 domain of Pgn (Cys^{358}−Cys^{435}), generated as fragment Val^{355}−Ala^{440} of Pgn; K5, kringle 5 domain of Pgn (Cys^{462}−Cys^{541}), generated as fragment Val^{449}−Phe^{546} of Pgn; K_a, equilibrium association constant; LBS, lysine binding site of Pgn; Ni^{2+}-NTA/agarose, nickel(2+) nitrilotriacetic acid−agarose; PCR, polymerase chain reaction; RP-HPLC, reversed-phase HPLC; r-A2PIC, generated recombinant wild-type A2PIC (Asn^{398}−Lys^{452}); r-A2PICmut, mutated C-terminal peptide of A2PI (Asn^{398}−Lys^{452}/Lys452Ala).

10.1021/bi026917n CCC: $25.00
Published on Web 01/10/2003

Scheme 1: Multiple Sequence Alignment of Human (*3*), Bovine (*37*), and Murine (*38*) A2PIC[a]

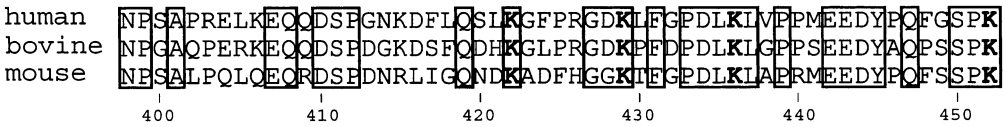

[a] Strictly conserved residues (lysines in boldface) are enclosed in boxes. Residue numbering follows the human A2PI sequence.

tion of a noncovalent complex between A2PIC and Plm kringles, which underscores the physiological relevance of this interaction.

Human A2PIC contains six lysine residues, including the C-terminus, Lys[452]. It is well-known that carboxylate-unblocked Lys residues bind to kringles with more affinity than the corresponding blocked lysines, suggesting that Lys[452] could mediate the interaction between kringles and A2PI. Indeed, a synthetic peptide corresponding to the C-terminal 26 amino acids of A2PI hinders reversible formation of the A2PI−Plm complex, presumably via competitive binding to the kringle domains (*5*, *6*). Removal of the C-terminal lysine residue with carboxypeptidase or substitution with arginine was found to diminish the interaction between these polypeptides and Plm (*6*, *12*).

Here we functionally and structurally characterize the intact A2PIC. Following standard recombinant DNA protocols, both the wild-type r-A2PIC (Asn[398]−Lys[452]) and a version of A2PIC mutated at the C-terminus, r-A2PICmut (Asn[398]−Lys[452]/Lys452Ala), were cloned and expressed in *Escherichia coli*. Qualitative structural features of r-A2PIC were assessed via NMR and circular dichroism (CD) spectroscopy, and binding affinities of Pgn kringles to both peptides were measured by intrinsic fluorescence ligand titrations. Finally, the docking of r-A2PIC to kringles was characterized on the basis of perturbations of K4 aromatic ^{1}H NMR signals in response to the presence of r-A2PIC and r-A2PICmut, confirming that the binding involves the canonical lysine-binding site (LBS).

MATERIALS AND METHODS

Materials. Calf intestinal alkaline phosphatase and restriction endonucleases were purchased from Boehringer Mannheim. *Pfu* DNA polymerase was obtained from Stratagene; T4 polynucleotide kinase and T4 DNA ligase were obtained from Promega. Nickel(2+) nitrilotriacetic acid−agarose (Ni^{2+}-NTA/agarose), the QIAprep spin miniprep kit, and the QIAquick gel extraction kit were purchased from QIAGEN. Agarose and acrylamide were obtained from Bio-Rad. Sephadex G-50sf and HiPrep 26/10 desalting were purchased from Pharmacia. FXa was obtained from Hematology Technologies Inc. (Essex Junction, VT).

Bacterial Strains and Plasmids. E. coli strain M15 (F^- Str^R *lacZ*^{del}) (*13*) was purchased from QIAGEN and used for routine transformation, plasmid preparation, and expression of r-A2PIC and r-A2PICmut. Plasmid pQE-8 utilized for the expression of r-A2PIC and r-A2PICmut was obtained from QIAGEN. The vector contains the regulating *E. coli* bacteriophage T5 promotor/*lac* operator element N250PSN250P29, a synthetic ribosomal binding site RBS II, and the phage λ transcription terminator t_0, encoding β-lactamase, and fuses an N-terminal hexahistidine tag to the recombinant protein (*14*). Plasmid pREP4 (QIAGEN) expresses high levels of the *lac* repressor and confers kanamycin resistance. Plasmid pSVIIPI, which contains the complete cDNA sequence of A2PI, was kindly provided by Prof. N. Aoki (Medical and Dental University of Tokyo, Japan).

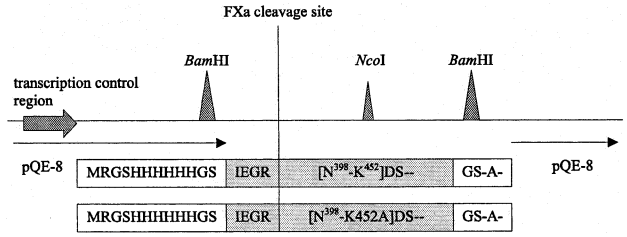

FIGURE 1: Expression vector constructs for r-A2PIC and r-A2PICmut. The indicated *Bam*HI endonuclease restriction sites, the FXa sensitive cleavage site (IEGR), and two stop codons were introduced by the corresponding 5′- and 3′-PCR primers. Directionality of the inserts was confirmed by *Nco*I. The mutation Lys452Ala was inserted by a 3′ mismatch primer.

DNA Manipulations. Plasmid isolations were carried out according to the QIAprep spin miniprep kit manual. Synthesis of oligonucleotides and DNA sequencing were performed by Microsynth (St. Gallen, Switzerland). DNA fragments generated by restriction endonucleases were purified on 2% agarose gels. DNA fragments were visualized by ethidium bromide and recovered from the gel by the QIAquick gel extraction kit according to the supplier's instructions.

Construction of the Expression Vector for r-A2PIC. The cDNA fragment corresponding to the A2PI sequence Asn[398]−Lys[452] was amplified from pSVIIPI by polymerase chain reaction (PCR). The PCR 5′-primer 5′-CGCGGGATCCA-TCGAGGGTAGAAACCCCAGTGCACC-3′, complementary to a segment of the noncoding A2PI cDNA, was employed to introduce a *Bam*HI restriction endonuclease site and the DNA segment coding for the coagulation factor Xa-sensitive (FXa) recognition site upstream of the codon for Asn[398]. The PCR 3′-primer 3′-GTCAAACCGTCGGGGT-TCATTATCCCTAGGGCGC-5′, which interacts within a region of the coding strand of the A2PI cDNA, was used to introduce two stop codons and a *Bam*HI restriction endonuclease site upstream of the codon for Lys[452].

The amplified r-A2PIC cDNA fragment was cleaved with *Bam*HI, cloned into *Bam*HI-cleaved and dephosphorylated pQE-8, and transformed into *E. coli* strain M15 containing the repressor plasmid pREP4. The direction of the insert was determined by digestion with *Nco*I (Figure 1). The insert was sequenced using the chain termination method (Microsynth, St. Gallen, Switzerland).

Construction of the Expression Vector for r-A2PICmut. The cloning strategy in *E. coli* strain M15 of r-A2PICmut was similar to the described method for r-A2PIC, except for the PCR 3′-mismatch primer 3′-GTCAAACCGTCGGGGC-GAATTATCCCTAGGGCGC-5′, which was employed to introduce the mutation Lys452Ala.

RP-HPLC. RP-HPLC was carried out on a Hewlett-Packard liquid chromatograph 1090 using an Aquapore butyl

column (2.1 mm × 100 mm, wide pore, 30 nm, 7 μm; Applied Biosystems). A linear acetonitrile gradient (0−100% solution B in 60 min) was used at a flow rate of 0.3 mL/min with 0.1% (by volume) trifluoroacetic acid in water for solution A and 0.1% (by volume) trifluoroacetic acid and 80% (by volume) acetonitrile in water for solution B.

Amino Acid Analysis. Samples were hydrolyzed in the gas phase with 6 M hydrochloric acid containing 0.1% (v/v) phenol for 24 h at 115 °C under vacuum. The liberated amino acids were left to react with phenyl isothiocyanate, and the resulting phenylthiocarbamyl amino acids were analyzed by RP-HPLC on a Nova Pak C_{18} column (4 μm, 3.9 mm × 150 mm; Waters) with a Hewlett-Packard liquid chromatograph 1090 equipped with an automatic injection system according to Bidlingmeyer (*15*). The corresponding ammonium acetate buffer replaced the 0.14 M sodium acetate buffer, pH 6.4.

Sequence Analysis. The N-terminal sequence analysis was carried out using Edman degradation in a pulsed-liquid-phase sequenator 477A from Applied Biosystems. The released amino acids were analyzed on-line by RP-HPLC.

Mass Spectrometry. The mass of the expressed constructs was determined by electrospray ionization mass spectrometry (ESI-MS) (VG platform mass spectrometer, Micromass Instruments, Manchester, U.K.).

Expression and Isolation of r-A2PIC and r-A2PICmut. The *E. coli* cells were grown at 37 °C in 2 × YT medium (100 μg of ampicillin/mL, 25 μg of kanamycin/mL) in 2 L round-bottomed flasks to an OD_{600} of about 0.7−0.9. To induce the production of the recombinant proteins, isopropyl thio-β-D-galactopyranoside was added to a final concentration of 2 mM. Cells were grown for an additional 3.5 h at 37 °C and finally harvested by centrifugation for 30 min (4000*g* at 4 °C). For obtaining the ^{15}N-labeled proteins, *E. coli* cells were grown in M9 medium containing [^{15}N]ammonium chloride. The cell pastes were stored at −80 °C until use. The relative amounts of the expression were determined by SDS−PAGE (15%). The proteins were made visible by Coomassie blue staining. A preliminary identification of the recombinant proteins by SDS−PAGE showed a main band indicating a relatively high level of expression. To isolate recombinant A2PIC and A2PICmut, the thawed cell pastes were suspended in extraction buffer, 6 M guanidine hydrochloride in 0.1 M sodium phosphate, pH 8 (5 mL/g of cell paste), stirred overnight at 4 °C, and centrifuged (15000*g* at 4 °C). The supernatants were loaded onto a Ni^{2+}-NTA/agarose column (1.5 × 5 cm) equilibrated with extraction buffer, pH 8. After successive washes with extraction buffer, pH 8 and 6.3, the recombinant proteins were eluted from the columns with extraction buffer, pH 5 (Figure 2A), yielding 4 mg/g of wet cells for both r-A2PIC and r-A2PICmut. Desalting of the proteins was performed on a prepacked HiPrep 26/10 desalting column, equilibrated with 20 mM ammonium hydrogen carbonate, and finally the proteins were lyophilized for storage. At this stage, before the removal of the His tag, r-A2PIC and r-A2PICmut eluted as sharp, symmetrical peaks upon RP-HPLC on an Aquapore butyl column. The molecular mass of 8024.58 ± 0.34 Da for r-A2PIC and 7968.25 ± 0.67 Da for r-A2PICmut corresponded well with the calculated value of 8.025.95 and 7968.86 Da, respectively. The amino acid analyses were also in good agreement with the expected values.

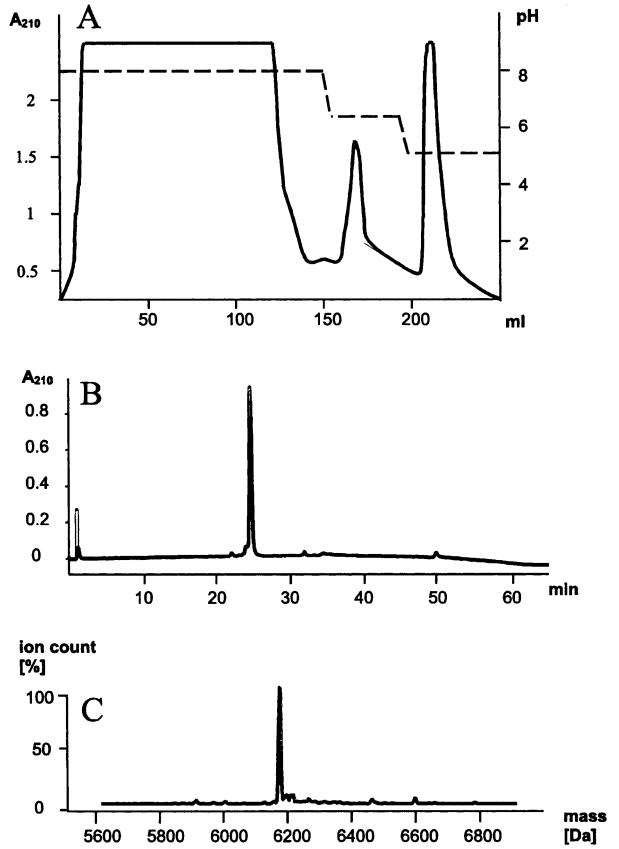

FIGURE 2: Chromatographic purification and mass spectrometry characterization of r-A2PIC. (A) Ni^{2+}-NTA chelate affinity chromatography. A crude extract of r-A2PIC was loaded on a Ni^{2+}-NTA/agarose column (1.5 × 5 cm) at pH 8 with a flow rate of 1 mL/min and eluted at pH 5.0. (B) RP-HPLC. r-A2PIC was analyzed on an Aquapore butyl column (2.1 mm × 100 mm, wide pore, 30 nm, 7 μm) using a linear acetonitrile gradient. (C) Positive ESI-MS of r-A2PIC (calculated mass: 6171.95 Da) dissolved in water/acetonitrile (1:1 v/v) containing 0.5% formic acid.

Removal of the His Tag. The His tag in r-A2PIC and r-A2PICmut was cleaved off by incubation with FXa for 16 h at 37 °C in 50 mM Tris-HCl (pH 8) containing 100 mM sodium chloride (enzyme to substrate ratio of 1:100, by mass). The cleaved proteins were separated from the His tag on a column of Sephadex G-50sf (2.5 cm × 100 cm) equilibrated with 50 mM ammonium hydrogen carbonate.

Intrinsic Fluorescence Titration. The effect of the ligands r-A2PIC and r-A2PICmut on the intrinsic fluorescence of different Pgn kringles was measured in 50 mM sodium phosphate, pH 8, at 25 °C with a Perkin-Elmer LS 50 B luminescence spectrometer (*16*). The concentration of the ligand in a 5 μM kringle solution was enhanced in 1, 5, 100, or 250 μM steps depending on the binding affinity of the investigated kringle until the change of intrinsic fluorescence was constant. Fluorescence was measured at 340 nm with excitation at 298 nm. K_a values were determined according to Scatchard (*17*).

Circular Dichroism Spectroscopy. Far-UV CD spectroscopic data were recorded on a Jasco J-715 spectropolarimeter equipped with a PFD 350S Peltier-type temperature controller and calibrated with (+)-10-camphorsulfonic acids (Aldrich). Quartz (1 mm) cuvettes (Starna) were used for all experiments. Protein concentrations were determined according to Pace (*18*). Secondary structure content was

estimated using CDsstr (*19*) with seven additional denatured proteins included in the basis set (*20*).

NMR Spectroscopy. NMR time-domain data were quadrature-detected on Bruker Avance DRX spectrometers equipped with triple-resonance *z*-gradient probes at 500 or 600 MHz as indicated. Data were processed with FELIX 98 (Accelrys).

$^1H-^2H$ exchange of r-A2PIC backbone amide protons was monitored by recording a series of 1D spectra at 21°C, 500 MHz, after the sample was dissolved in 500 μL of ^2H_2O at a concentration of ~0.4 mM, pH* ~5.8, until exchange was complete. As a control, data were recorded for r-A2PIC dissolved in ~500 μL of 90% ^1H_2O/10% ^2H_2O, pH 5.2.

For monitoring the response of kringle aromatic residues to ligands, K4 samples were incubated at 37 °C for 3 h in ^2H_2O to exchange labile hydrogen atoms for deuterons. After lyophilization, the samples were dissolved in 500 μL of ^2H_2O at a concentration of ~0.5 mM, and the pH* was adjusted to 7.2 with ^{2}HOAc or NaO^{2}H. Ligand complexation experiments shown in Figure 4 were performed at 43 °C, 500 MHz, by adding small aliquots of 5−75 mM stock solution of ligand dissolved in ^2H_2O. The response of A2PIC to r-K1 or K4 binding was monitored via $^1H-^{15}N$ HSQC on an ^{15}N-labeled r-A2PIC sample, dissolved in 500 μL of 90% ^1H_2O/10% ^2H_2O.

RESULTS

Recombinant A2PIC and A2PICmut Expression. Both r-A2PIC (Figure 2B) and r-A2PICmut eluted as sharp, symmetrical peaks on RP-HPLC. After removal of the His tag, the measured masses of 6171.69 ± 0.15 Da for r-A2PIC (Figure 2C) and 6113.93 ± 0.21 Da for r-A2PICmut closely agree with the calculated values of 6171.95 and 6114.85 Da, respectively. N-Terminal analyses yielded the expected Asn-Pro-Ser-Ala-Pro sequence for each construct.

Secondary Structure of r-A2PIC. All backbone amide NMR signals in the 1D ^{1}H spectrum (Figure 3A, trace a) lie within the range $7.7 < \delta_H < 8.7$ ppm. Such chemical shifts and low spectral dispersion of the H^N resonances are typical of nonglobular proteins. Upon dissolution of r-A2PIC in ^2H_2O, only one H^N peak at ~8.09 ppm remained detectable at ~6 min (Figure 3A, trace b), and by ~24 min (Figure 3A, trace c) all amides were fully deuterated. The relatively fast exchange indicates that, on the experimental time scale, the peptidyl amides are solvent exposed, consistent with negligible internal H-bonding and/or steric shielding.

Figure 3B displays the far-UV CD spectra of r-A2PIC. Consistent with the NMR evidence, the negative band at ~200 nm in the far-UV CD spectrum of r-A2PIC (Figure 3B, trace d) is characteristic of unfolded, flexible polypeptides (*20*, *21*). Analysis of the spectrum via CDsstr (*19*) indicates approximately 1% α-helix, 8% 3_1-helix, 4% 3_{10}-helix, 14% β-strand, 9% β-turns, and 64% "other", hinting at only a small degree of regular secondary structure. Varying the temperature between 25 and 95 °C in five steps reveals an isodichroic point at ~212 nm (Figure 3B, traces d and f), which suggests a two-state temperature-dependent transition. After allowing the protein solution to cool from 95 to 25 °C, the spectrum is measurably different from the one originally recorded at 25 °C (Figure 3B, trace e), revealing some structural change. The combined CD and NMR evidence (Figure 3) thus suggests that r-A2PIC is not a compact, folded globular domain but rather a flexible polypeptide of low β-structure.

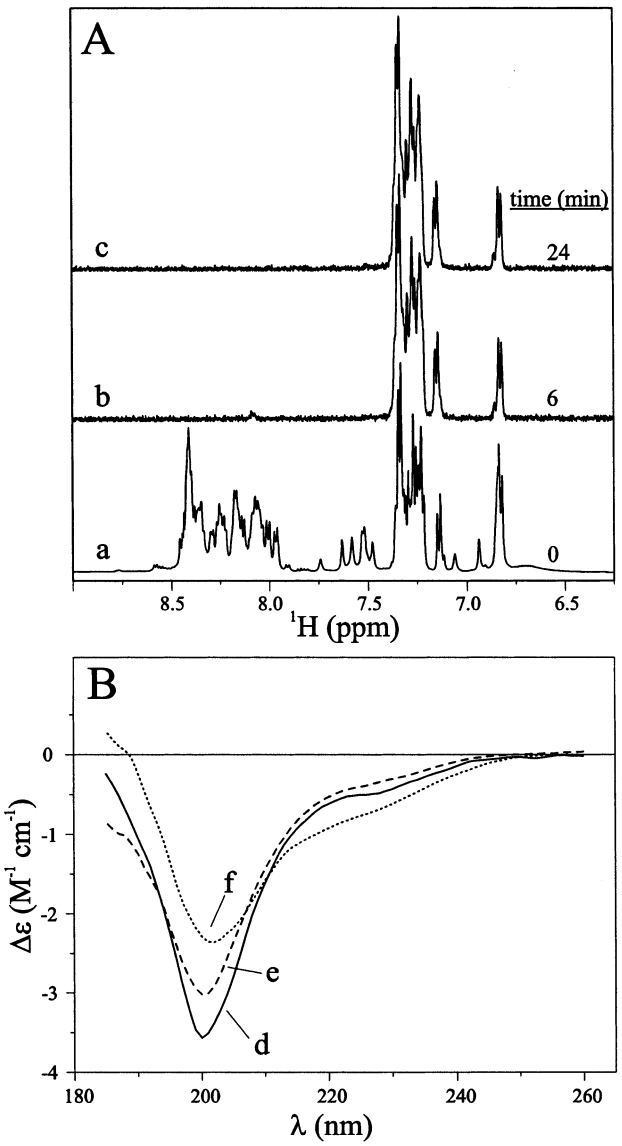

FIGURE 3: 500 MHz ^{1}H NMR (A) and far-UV CD (B) spectra of r-A2PIC. For the control NMR spectrum (a), the sample was dissolved to ~1 mM in 10%/90% $^2H_2O/^1H_2O$, recorded at pH 5.2, 27 °C. Spectra b and c were recorded ~6 and ~24 min, respectively, after sample was dissolved in 100% ^2H_2O, pH 5.8, 21 °C. Water suppression was accomplished via presaturation and time-domain convolution (*43*). CD spectra were recorded using a 1 mm cell at 25 °C (d), 95 °C (f), and 25 °C (e); the protein concentration was ~12 μM in 10 mM TES and 50 mM NaF, pH 8.0. Spectrum e was recorded on the sample that generated spectrum f after gradual cooling.

Binding of r-A2PIC to Kringles. Except for K3 (*22*, *23*), Pgn kringles variously exhibit lysine-binding capability. From inhibitory studies on Plm it has been proposed that the A2PI interaction with Plm is mediated by the A2PIC C-terminal Lys^{452} which would anchor to the canonical kringle lysine-binding site (LBS) (*4*, *6*). To verify this hypothesis, we measured, via intrinsic fluorescence ligand titrations, the affinities of Pgn kringles for r-A2PIC. The corresponding equilibrium association constant (K_a) values were estimated by least-squares fitting the linearized Langmuir adsorption isotherms. We find that r-A2PIC interacts most strongly with r-K1 ($K_a = 70 \pm 7$ mM^{-1}) and K4 (46 ± 5 mM^{-1}) and to

Table 1: Kringle Binding Affinities[a]

	ligand				
kringle	r-A2PIC	AcLys	6-AHA	r-A2PICmut	AcLysOMe
r-K1	70 ± 7	41 ± 2[b]	75 ± 11	11.6 ± 0.5	$0.16 \pm 0.00_5$[b]
r-K2	3.2 ± 0.5	0.96 ± 0.11[c]	2.7 ± 0.1		
r-K3mut	~4		4.2 ± 0.1[e]		
K4	46 ± 5	37 ± 1[d]	36 ± 9	9.1 ± 0.2	~0.2 [f]
K5	4.3 ± 1.9	0.18 ± 0.01[c]	3.8 ± 0.7		

[a] K_a (mM^{-1}). [b] From ref *29*. [c] From ref *23*. [d] From ref *28*. [e] From ref *24*. [f] From ref *30*.

a lesser extent with r-K2 (3.2 ± 0.5 mM^{-1}) and K5 (4.3 ± 1.9 mM^{-1}).

As a control we also determined the K_a's for the antifibrinolytic drug 6-aminohexanoic acid (6-AHA), a lysine-type compound, one of the strongest simple linear ligands known (*23*). The estimated values (Table 1) for K4 ($K_a = 36 \pm 9$ mM^{-1}) and K5 (3.8 ± 0.7 mM^{-1}) are consistent with those determined via ^1H NMR titrations (21 ± 1 mM^{-1} and 10.6 ± 0.2 mM^{-1}, respectively) (*25*, *26*). Similarly, the obtained K_a's for r-K1 (75 ± 11 mM^{-1}) and r-K2 (2.7 ± 0.1 mM^{-1}) closely match reported values deduced from fluorescence (*16*, *27*) (77 mM^{-1} and 1.79 ± 0.10 mM^{-1}, respectively) and ^1H NMR titration experiments (*23*) (74.2 ± 8 mM^{-1} and 2.3 ± 0.2 mM^{-1}, respectively). Although wild-type K3 is not endowed with a functional LBS, the Lys311Asp mutant (r-K3mut) exhibits lysine-binding capability and interacts measurably with 6-AHA ($K_a = 4.2 \pm 0.1$ mM^{-1}) (*24*). Consistent with these results, we observe that the r-K3mut shows an affinity for r-A2PIC ($K_a \sim 4$ mM^{-1}).

To gauge the significance of the above data, Table 1 also includes K_a values for N^{α}-acetyllysine (AcLys), a ligand that models C-terminal lysines, previously determined via ^1H NMR (*23*, *28*, *29*). As is the case with r-A2PIC, AcLys binds to K1 ($K_a = 41 \pm 2$ mM^{-1}) and K4 (37 ± 1 mM^{-1}) and relatively more weakly to r-K2 (0.96 ± 0.11 mM^{-1}) and K5 (0.18 ± 0.01 mM^{-1}). Thus, r-A2PIC and 6-AHA exhibit comparable kringle-binding affinities that are somewhat higher than those measured for AcLys.

Binding of r-A2PICmut to Kringles. To discriminate the role of the C-terminus, Lys^{452}, the binding of r-A2PICmut (Lys452Ala) to r-K1 and K4 was also investigated. Comparing the K_a values of r-A2PIC and r-A2PICmut for r-K1 (70 ± 7 mM^{-1} and 11.6 ± 0.5 mM^{-1}, respectively) and K4 (46 ± 5 mM^{-1} and 9.1 ± 0.2 mM^{-1}, respectively) reveals that the $Lys^{452} \rightarrow$ Ala replacement yields an approximate 5-fold decrease in the affinity of A2PIC for both kringles.

Hence, although the C-terminal Lys^{452} is the main determinant of the affinity of r-A2PIC for kringles, r-A2PICmut retains a significant binding capability toward these modules. To assess the relative contribution of this interaction, we compare these results against the binding constants for N^{α}-acetyllysine methyl ester (AcLysOMe), a mimic of internal Lys residues. It is noteworthy that AcLysOMe binds r-K1 ($K_a = 0.16 \pm 0.00_5$ mM^{-1}) and K4 (~ 0.2 mM^{-1}) (*29*, *30*) approximately an order of magnitude more weakly[2] than A2PICmut.

Kringle Docking of r-A2PIC. The response of the K4 ^1H NMR signals to lysine-type ligands has been studied extensively and the constellation of aromatic side chains involved in the interaction, namely, Trp^{25}, Trp^{62}, Phe^{64}, Trp^{72}, and Tyr^{74}, established (*23*, *31*−*34*). This provides a platform to investigate via ^1H NMR the perturbations of the K4 aromatic groups in response to AcLys, r-A2PIC, and r-A2PICmut.

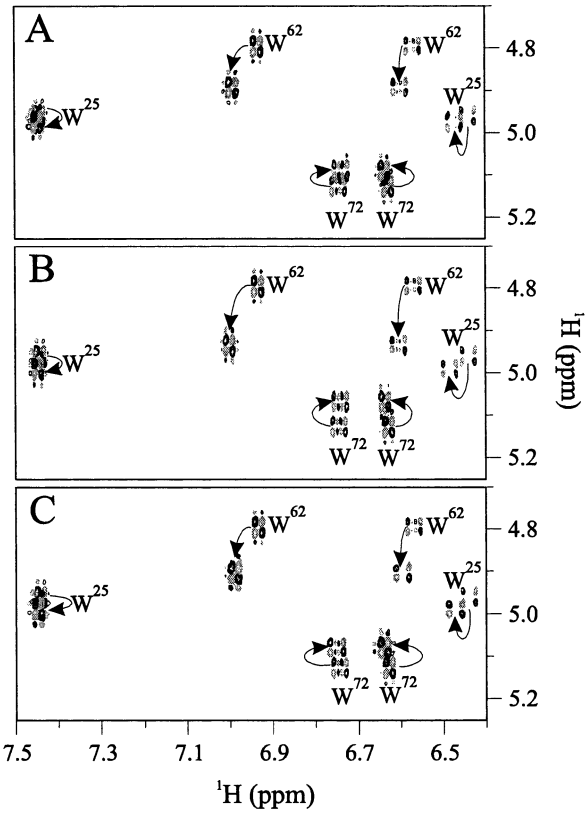

FIGURE 4: 500 MHz ^1H NMR phase-sensitive COSY of K4: ligand effects on the Trp aromatic rings. Spectra of ligand-bound K4 are superimposed on that of ligand-free K4: ± AcLys (A), ± r-A2PIC (B), and ± r-A2PICmut (C). Cross-peak shifts are denoted by curved arrows. The ligand-free K4 sample was ~0.5 mM. Ligand-bound K4 samples were (A) ~0.5 mM [K4], [AcLys]/[K4] ~0.8, (B) ~0.4 mM [K4], [r-A2PIC]/[K4] ~0.8, and (C) ~0.29 mM [K4], [r-A2PICmut]/[K4] ~1.64. All spectra were recorded for samples dissolved in ^2H_2O, pH* 7.2, 43 °C.

Figure 4 shows expanded an area of the Trp aromatic region of the K4 ^1H NMR COSY spectrum. Upon docking AcLys (Figure 4A), r-A2PIC (Figure 4B), or r-A2PICmut

[2] Because of dilute solution conditions, the fluorescence binding assays on A2PIC and A2PICmut were conducted on samples dissolved in 50 mM sodium phosphate buffer, while the NMR assays for the AcLys and AcLysOMe binding were done at ~1 mM kringle concentration in the absence of buffer. Since the main component of the interaction with the kringles' LBS is electrostatic pairing of the ligand Lys cationic group to the Asp^{55} and Asp^{57} anionic side chains (*31*), the presence of buffer would be expected, if anything, to weaken the interaction between the kringle LBS and A2PIC or A2PICmut, reenforcing the trends noticed for the relative binding affinities.

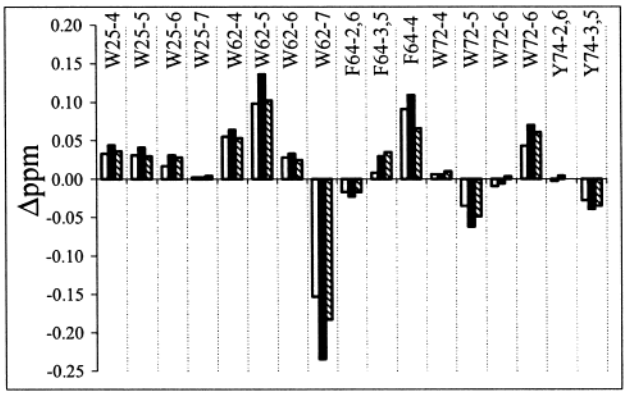

FIGURE 5: ^{1}H NMR shifts of representative kringle LBS aromatic signals that originate from binding AcLys (white bars), r-A2PIC (black bars), and r-A2PICmut (hatched bars). Data were extracted from COSY spectra (Figure 4).

(Figure 4C), each K4 Trp indole ring is perturbed in an essentially identical fashion. Indeed, as may be judged from Figure 5, the overall pattern of aromatic side chain resonance shifts induced by these ligands on the canonical K4 LBS is rather uniform. Furthermore, the perturbation is localized since spatially removed amino acids, such as Tyr^2, are impervious to the various tested ligands. Although other binding mechanisms can be envisioned, which do not require direct coupling via lysine side chains (*35*), the evidence (Figures 4 and 5), as well as that resulting from AcLysOMe binding (not shown; see ref *36*), unambiguously demonstrates that r-A2PIC (Figure 4B) and r-A2PICmut (Figure 4C) anchor to K4 similarly, namely, via interactions with the latter's LBS.

DISCUSSION

Intrinsic fluorescence ligand titrations (Table 1) identify r-A2PIC (Asn^{398}−Lys^{452}) as being a relatively high-affinity kringle ligand, comparable to the antifibrinolytic drug 6-AHA. A 5-fold decrease in the K_a values of r-A2PICmut (K452A) for r-K1 and K4 relative to r-A2PIC suggests that the C-terminal residue plays an important role in the kringle−ligand interaction. Binding AcLys, r-A2PIC, and r-A2PICmut induces changes in the chemical shift of the same key aromatic residues involved in the complexation by K4 of Lys-type ligands (Figures 4 and 5), indicating that all three ligands dock to kringles in a similar fashion. Consistently, when the LBS is reconstituted in K3 (as in the r-K3mut), the modified kringle binds A2PIC.

The primary structures of the bovine and murine A2PIC homologues (*37*, *38*) are known (Scheme 1). It is interesting that while all lysine-binding kringles in human Pgn are basic, the A2PIC pI values, as estimated from the sequences, are 4.7 (bovine) and 5.1 (murine), and 5.2 (human). Specifically, while at pH 7 the kringles carry an estimated positive charge of ∼0.9 eu for K1 and ∼4.0 eu for K4, all three A2PIC homologues carry a net negative charge (∼−3.9 eu for bovine, −1.9 eu for murine, and −1.0 eu for human), suggesting electrostatic complementarity in the binding interaction. In this context, physiological sulfonation of Tyr^{445} (*39*) should only enhance this effect.

The predicted effect of the cationic Lys^{452} side chain on the pI of human r-A2PIC cannot be ignored since the electric field originating from the ligand might be suspected to affect the kringle−ligand interaction. As a consequence of the Lys452Ala mutation, the r-A2PIC pI drops to 4.8 for r-A2PICmut which, in terms of electrostatic interaction with kringles, should *enhance* the K_a for the mutant. Since this predicted effect contradicts the observations, it strongly argues in favor of Lys^{452} directly anchoring to one of the kringles' LBS.

Both r-A2PIC and r-A2PICmut bind to the investigated kringles more strongly than the model lysine ligands AcLys and AcLysOMe (Table 1), hinting that, relative to arbitrary C-terminal or internal lysine residues, A2PIC may have evolved to optimize noncovalent interactions with the LBS. Such capability is likely to confer a functional advantage to A2PI: an upregulated kringle-binding capacity would help to ensure rapid inhibition of Plm and minimize competition

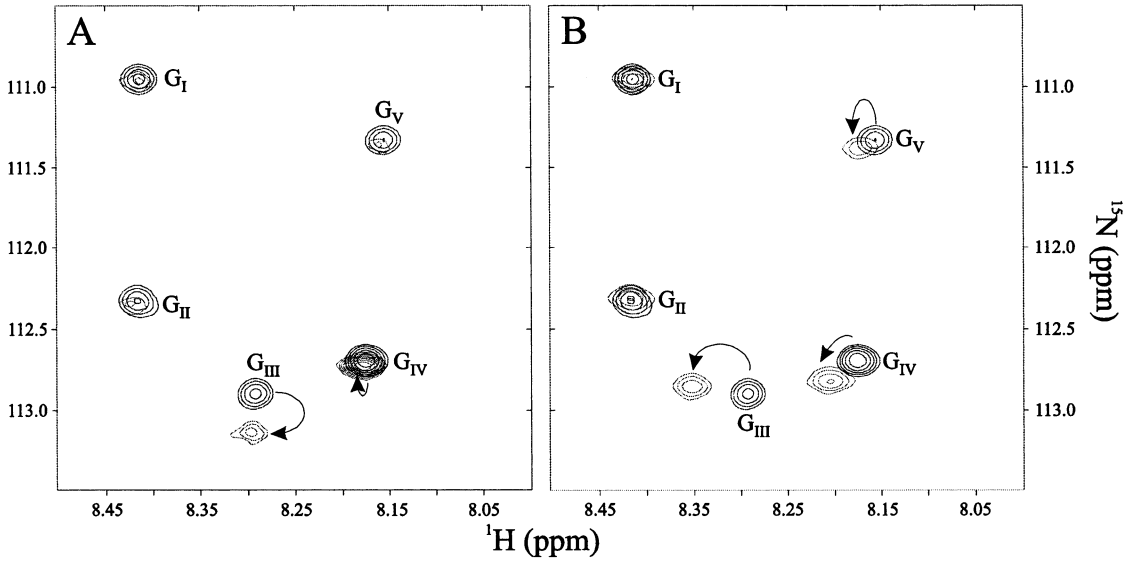

FIGURE 6: Glycine region ^{1}H−^{15}N HSQC of r-A2PIC: effect of r-K1 (A) and K4 (B) binding. Spectra of r-A2PIC (∼1 mM, pH ∼6.5) (dark contours) and r-A2PIC in the presence of an ∼3-fold excess of r-K1 (A) or of K4 (B) (light contours) are superimposed. Cross-peaks are arbitrarily labeled G_I−G_V and kringle-induced shifts denoted by curved arrows. Kringle samples were dissolved in 10% ^2H_2O, pH 7.2 (K1) or pH 6.5 (K4), and the spectra recorded at 27 °C, 14 T.

from arbitrary peptides with Lys residues. At least one other physiological kringle-binding peptide seems to have adopted this strategy as well, the N-terminal PAN domain of Pgn. This domain influences the global fold and activity of Pgn (*40*). We have demonstrated elsewhere (*36*, *41*) that a structured CNBr cleaved fragment, $Glu^{1}-HSer^{57}$, interacts with lysine-binding kringles most likely via Lys^{50}. Specifically, $Glu^{1}-HSer^{57}$ binds to r-K1 ($K_a \sim 4.6$ mM^{-1}) and K4 ($\sim$6.2 mM^{-1}) with greater affinity than AcLysOMe [$K_a \sim 0.16$ and $\sim$0.2 mM^{-1}, respectively (*29*, *30*)] and even, in the case of K4, than the PAN-derived peptide fragment 44−52 ($K_a \sim 1.4$ mM^{-1}), which encompasses Lys^{50} (*36*). Hence both the PAN domain of Pgn and the A2PICmut exhibit enhanced kringle-binding capacity relative to an arbitrary internal Lys residue, suggesting effects encoded by the amino acid sequence.

Structurally, on the basis of the CD and NMR evidence (Figure 3), r-A2PIC is not a globular domain but rather a loosely structured polypeptide with at most $\sim$10% β structure. This is consistent with a lack of cystine bridges restricting the folding. The biological significance of this result is unclear but suggests a degree of structural plasticity that would enable A2PIC to adapt to the surface exposed by the Plm heavy chain linear multikringle array. Indeed, preliminary NMR $^{1}H-^{15}N$ HSQC experiments on ^{15}N-labeled r-A2PIC show a number of amide NH signals responding to the presence of r-K1 and K4. Focusing on the glycine cross-peaks, the addition of excess r-K1 or K4 (Figure 6) perturbs all five Gly NH resonances, with the most significant shifts observed for the cross-peaks labeled G_{III}, G_{IV}, and G_V. Since the C-terminal Lys^{452} critically mediates docking to the binding pocket, one may have anticipated that perhaps one Gly signal, corresponding to Gly^{449}, would become perturbed upon addition of K4. Hence, it is revealing that three glycyl HN resonances respond to kringle presence. All five glycines (413, 423, 427, 432, and 449) are sequentially proximal to at least one lysine residue (415, 422, 429, 436, and 452). Therefore, shifts in three peaks may result from the anchoring of the C-terminus and at least two of the interior five lysines to the LBS.

Interestingly, among the human, bovine, and murine A2PIC primary structures, 26 out of 55 residues are strictly conserved (Scheme 1). Of the six Lys residues in the human A2PIC, those at sites 422, 429, and 436 and at the C-terminus, 452, are found in all three sequences yielding 4/6 = 67% conservancy, significantly higher than the 26/55 = 47% that characterizes the entire polypeptide. Assuming that these residues are conserved because of function, it is tempting to speculate that the four Lys residues may be involved in the interaction with Plm. This would be consistent with the number of lysine-binding kringles present in the Plm heavy chain and is in line with the hypothesis that physiologically, to rapidly inhibit Plm, A2PI has evolved the ability to hitch to several kringles via multiple sites at the C-terminal tail. Indeed, for a fully extended linear A2PIC, the distance between the last two lysines, Lys^{436} and Lys^{453} (Scheme 1), is $\sim$30 Å, which would match the "bite" required to bridge the LBSs' of kringles 1 and 2 as estimated from the kringle 1 + 2 + 3 crystal structure (*42*), where the distance from Trp^{144} (K1 LBS) to Trp^{225} (K2 LBS) is also $\sim$30 Å. Along these lines, one may further speculate that the highly electronegative, sulfonated EEDY*445 segment of A2PIC, distanced six residues from Lys^{452} at the C-terminus, may, in turn, provide a rather specific site for interacting with a basic patch on the surface of a kringle, possibly K3, the only non-lysine binding Plm kringle, or K4, whose estimated electrostatic charges at pH 7 are $\sim$3.1 and $\sim$4.0 eu, respectively.

CONCLUSIONS

Overall, r-A2PIC is flexible, which would enable A2PI to adapt its folding in order to interact with the Plm heavy chain multikringle array. As discussed above, local structural features modulate the affinity of Lys residues in A2PIC for kringles so that the wild-type r-A2PIC may use internal Lys residues to strengthen the binding mediated by the C-terminus Lys^{452} in a cooperative, zipper-like fashion. In this context, it is interesting to notice that the affinity of r-A2PIC for r-K1 is $\sim$1.5 times larger than for K4, while in the case of r-A2PICmut the affinities for the two kringles are about equal and substantially lower than that exhibited by the wild-type A2PIC. This suggests that the C-terminus of A2PIC could favor initial binding to K1 and that subsequent interactions via internal lysines might involve K4 followed by K2 and K5.

ACKNOWLEDGMENT

We thank Mr. U. Kämpfer for expert technical support and Prof. R. Gil for valuable assistance with the NMR experiments.

REFERENCES

1. Tordai, H., Bányai, L., and Patthy, L. (1999) *FEBS Lett. 461*, 63−67.
2. Shieh, B. H., and Travis, J. (1987) *J. Biol. Chem. 262*, 6055−6059.
3. Tone, M., Kikuno, R., Kume-Iwaki, A., and Hashimoto-Gotoh, T. (1987) *J. Biochem. (Tokyo) 102*, 1033−1041.
4. Wiman, B., Lijnen, H. R., and Collen, D. (1979) *Biochim. Biophys. Acta 579*, 142−154.
5. Sasaki, T., Morita, T., and Iwanaga, S. (1986) *J. Biochem. (Tokyo) 99*, 1699−1705.
6. Hortin, G. L., Gibson, B. L., and Fok, K. F. (1988) *Biochem. Biophys. Res. Commun. 155*, 591−596.
7. Wiman, B., Boman, L., and Collen, D. (1978) *Eur. J. Biochem. 87*, 143−146.
8. Kluft, C., Los, P., Jie, A. F., van Hinsbergh, V. W., Vellenga, E., Jespersen, J., and Henny, C. P. (1986) *Blood 67*, 616−622.
9. Clemmensen, I., Thorsen, S., Mullertz, S., and Petersen, L. C. (1981) *Eur. J. Biochem. 120*, 105−112.
10. Christensen, U., and Clemmensen, I. (1977) *Biochem. J. 163*, 389−391.
11. Wiman, B., and Collen, D. (1978) *Eur. J. Biochem. 84*, 573−578.
12. Hortin, G. L., Trimpe, B. L., and Fok, K. F. (1989) *Thromb. Res. 54*, 621−632.
13. Kwon, K. S., Kim, J., Shin, H. S., and Yu, M. H. (1994) *J. Biol. Chem. 269*, 9627−9631.
14. Hochuli, E., Bannwarth, W., Döbeli, H., Gentz, R., and Stüber, D. (1988) *Biotechnology (New York) 213*, 1321−1325.
15. Bidlingmeyer, B. A., Cohen, S. A., and Tarvin, T. L. (1984) *J. Chromatogr. 336*, 93−104.
16. Menhart, N., Sehl, L. C., Kelley, R. F., and Castellino, F. J. (1991) *Biochemistry 30*, 1948−1957.
17. Scatchard, G. (1948) *Ann. N.Y. Acad. Sci. 51*, 660−672.
18. Pace, C. N., Vajdos, F., Fee, L., Grimsley, G., and Gray, T. (1995) *Protein Sci. 4*, 2411−2423.
19. Johnson, W. C. (1999) *Proteins 35*, 307−312.
20. Venyaminov, S., Baikalov, I. A., Shen, Z. M., Wu, C. S., and Yang, J. T. (1993) *Anal. Biochem. 214*, 17−24.

21. Greenfield, N., and Fasman, G. D. (1969) *Biochemistry 8*, 4108−4116.
22. Söhndel, S., Hu, C. K., Marti, D., Affolter, M., Schaller, J., Llinás, M., and Rickli, E. E. (1996) *Biochemistry 35*, 2357−2364.
23. Marti, D. N., Hu, C. K., An, S. S., von Haller, P., Schaller, J., and Llinás, M. (1997) *Biochemistry 36*, 11591−11604.
24. Bürgin, J., and Schaller, J. (1999) *Cell Mol. Life Sci. 55*, 135−141.
25. Thewes, T., Constantine, K., Byeon, I. J., and Llinás, M. (1990) *J. Biol. Chem. 265*, 3906−3915.
26. Rejante, M. R., Byeon, I. J., and Llinás, M. (1991) *Biochemistry 30*, 11081−11092.
27. Nilsen, S. L., Prorok, M., and Castellino, F. J. (1999) *J. Biol. Chem. 274*, 22380−22386.
28. De Marco, A., Petros, A. M., Laursen, R. A., and Llinás, M. (1987) *Eur. Biophys. J. 14*, 359−368.
29. Rejante, M. R. (1992) Proton NMR studies on the structure and ligand-binding properties of human plasminogen kringles 1 and 4, Doctoral Dissertation, Carnegie Mellon University, Pittsburgh, PA.
30. Petros, A. M., Ramesh, V., and Llinás, M. (1989) *Biochemistry 28*, 1368−1376.
31. Tulinsky, A., Park, C. H., Mao, B., and Llinás, M. (1988) *Proteins 3*, 85−96.
32. Hochschwender, S. M., and Laursen, R. A. (1981) *J. Biol. Chem. 256*, 11172−11176.
33. Ramesh, V., Petros, A. M., Llinás, M., Tulinsky, A., and Park, C. H. (1987) *J. Mol. Biol. 198*, 481−498.
34. Thewes, T., Ramesh, V., Simplaceanu, E. L., and Llinás, M. (1988) *Eur. J. Biochem. 175*, 237−249.
35. Rios-Steiner, J. L., Schenone, M., Mochalkin, I., Tulinsky, A., and Castellino, F. J. (2001) *J. Mol. Biol. 308*, 705−719.
36. An, S. S., Carreño, C., Marti, D. N., Schaller, J., Albericio, F., and Llinás, M. (1998) *Protein Sci. 7*, 1960−1969.
37. Christensen, S., Berglund, L., and Sottrup-Jensen, L. (1994) *FEBS Lett. 343*, 223−228.
38. Menoud, P. A., Sappino, N., Boudal-Khoshbeen, M., Vassalli, J. D., and Sappino, A. P. (1996) *J. Clin. Invest. 97*, 2478−2484.
39. Hortin, G., Fok, K. F., Toren, P. C., and Strauss, A. W. (1987) *J. Biol. Chem. 262*, 3082−3085.
40. Ponting, C. P., Marshall, J. M., and Cederholm-Williams, S. A. (1992) *Blood Coagulation Fibrinolysis 3*, 605−614.
41. An, S. S., Marti, D. N., Carreño, C., Albericio, F., Schaller, J., and Llinás, M. (1998) *Protein Sci. 7*, 1947−1959.
42. Abad, M. C., Arni, R. K., Grella, D. K., Castellino, F. J., Tulinsky, A., and Geiger, J. H. (2002) *J. Mol. Biol. 318*, 1009−1017.
43. Marion, D., Ikura, M., and Bax, A. (1989) *J. Magn. Reson. 84*, 425−430.

BI026917N